University of North Carolina Asheville
Journal of Undergraduate Research
Asheville, North Carolina
May 2019

Synthesis and Antibiotic Evaluation of Bedaquiline Analogs that Target ATP Synthase in *Escherichia coli*

Rayven Van Kalker
Chemistry Department
The University of North Carolina Asheville
One University Heights
Asheville, North Carolina 28804 USA

Faculty Advisor: Dr. Amanda Wolfe

Abstract

Emergence of drug-resistant bacteria represents a high, unmet medical need, and the added lack of antibacterial agents with novel mechanisms of action only compounds this issue. Treatability of Gram-negative bacteria, such as *Escherichia coli* (*E. coli*), is particularly difficult due to the addition of a thick outer membrane and high levels of molecular machinery such as drug efflux pumps. Therefore, innovative antibacterial mechanisms of action are greatly needed to combat this issue. ATP synthase has been validated as an antibacterial target in *Mycobacterium tuberculosis*, where its activity can be specifically blocked by the novel drug, Bedaquiline (BDQ). However, potency of BDQ is restricted to mycobacteria with little or no effect on the growth of other Gram-positive or Gram-negative bacteria. Here, we identify the differences in the ATP synthase amino acid sequence of each pathogen and synthesize analogs of BDQ that specifically target ATP synthase in *E. coli.* Using electrophilic aromatic substitution reactions, a variety of C2 BDQ analogs have been synthesized and evaluated for ATP synthase inhibition using an ATP-driven H^+ pumping assay in inside-out membrane vesicles. Three of these base analogs, one with a naphthalene substituent, another with a hydroxy, and the other with a N-dimethylaminopropanol, have shown activity toward both *E. coli* and *Staphylococcus aureus* within the 100-1000 μg/mL range and have since been further elaborated structurally at the C3 position. Development of the diarylquinolines class may represent a promising strategy for combating Gram-negative pathogens.

1. Introduction

The number of deaths due to bacterial infections is projected to reach 10 million by the year 2050, and currently, Gram-negative bacteria are responsible for one-half of all healthcare associated infections (HAIs), including the incidence of 1.7 million new cases of HAIs in the U.S. annually. One infamous Gram-negative bacterium, *Escherichia coli (E. coli),* currently causes approximately 100,000 new cases of bacterial infections annually, and is the leading cause of bloodstream infections. More importantly, the prevalence and acquisition of multidrug-resistant Gram-negative bacteria has surpassed that of vancomycin-resistant *Enterococci* and methicillin-resistant *Staphylococcus aureus*.[1] Gram-negative bacteria are more challenging to treat compared to Gram-positive due to the differences in the cell wall structures, with Gram-positive having thick peptidoglycan layers and Gram-negative having a thin peptidoglycan layer and an additional outer membrane.

Multidrug resistant (MDR) bacteria inevitably emerge after repeated misuse of antibiotics and broad spectrum drugs. When an infection is treated with an antibiotic, naturally resistant populations of bacteria, caused by spontaneous, genetic mutations, will remain to transfer their resistance traits to replicating bacterii. Infections that are caused by MDR Gram-negative bacteria are associated with up to five times higher mortality rates compared with infections that are caused by susceptible Gram-negative bacteria.[2] Because of these factors, new drugs are being researched and produced to combat MDR bacteria. However, efficient synthesis and mass-production of drugs for Gram-negative bacteria has been an ongoing challenge in the field of medicinal chemistry.

Diarylquinolines (DARQs) are a new class of compounds that demonstrate potent antibacterial activity on replicating *Bacilli*.[3] A representative compound from this class, Bedaquiline (BDQ) (also known as TMC-207 and R207910), was the first novel antitubercular drug approved by the US Food and Drug Administration (FDA) specifically for the treatment of multidrug resistant-tuberculosis (MDR-TB) in the past 40 years (Figure 1).[4] The current standard of treatment for TB includes combinations of multiple drugs over an extensive period of time to prevent drug resistance and bypass the outer membranes of the TB mycobacteria, *Mycobacterium tuberculosis* (*M. tb*). BDQ is able to bypass the outer layers of *M. tb.* and bind to the F_o c-ring subunit of ATP synthase. Inhibition of the c-ring stalls the proton pump mechanism and prevents ATP production which is essential for cell life.[2, 5] BDQ is effective against all states of *M. tb* including active, dormant, replicating, and non-replicating, and has no cross-resistance in the presence of other antibiotics.[6]

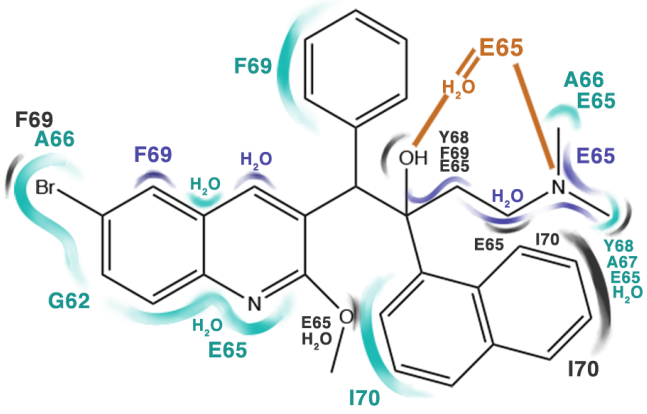

Figure 1. Two-dimensional (2D) illustration of BDQ's structure when in complex with M. tuberculosis including the key amino acid interactions with the c-ring at each position. Interaction distances, determined by Priess et. al., are color coded and include: H-bond, 2.5-2.6 A; Van der Waals (VdW) interactions, 3.0-3.5 A; VdW interactions, 3.5-4.0 A; VdW interactions, 4.0-4.5 A.

The mechanism of action of BDQ binding to the mycobacterial c-ring described by Preiss et. al. is illustrated by Figure 2. The ATP synthase F_o motor unit is shown from the cytoplasmic side, cut open at the level of the c-ring ion-binding sites.[7] One or more BDQ molecules approach the c-ring surface from the hydrophobic zone of the lipid bilayer. Each BDQ molecule binds to the region of the ion-binding site and interacts with one of the conserved polar residues such as Asp65. The dimethylamino group contacts the carboxyl group of the ion-binding aspartate (Figure 2). Depending on the strength of binding (ideally 2.5-2.6 Å), the bulky drug molecule will bind to the c-ring and be steriTcally and energetically disfavored to pass the a/c-ring interface. Thus, the rotor motion stalls ion exchange at the ATP synthase, and ATP synthesis activity stops.

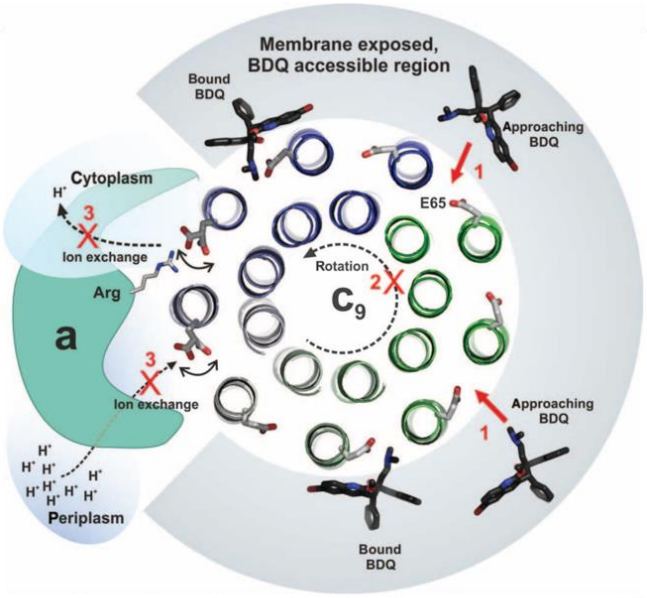

Figure 2. Top view of mycobacterial ATP synthase F_o motor unit.[7] Adapted from Preiss, L., et. al. Structure of the mycobacterial ATP synthase F_o rotor ring in complex with the anti-TB drug bedaquiline. *Sci. Adv.* **2015**, *1*, e1500106. © The Authors, some rights reserved; exclusive licensee. American Association for the Advancement of Science. Distributed under a Creative Commons Attribution NonCommercial License 4.0 (CC BY-NC).

In 2005, BDQ was confirmed to be capable of inhibiting 99% of the following pathogens with minimum inhibitory concentration (MIC) values ranging from 16-64 µg/mL, including the Gram-positive *Nocardia*, *Streptococcus pneumoniae*, *Staphylococcus aureus*, and *Enterococcus faecalis*, and the Gram-negative *Escherichia coli* and *Haemophilus influenzae*.[8] Previous efforts have been made to inhibit *E. coli* by other mechanisms of action including the inactivation of chromosomal genes and alteration to the cell wall and plasma membrane, among others. However, the F_o c-ring subunit of ATP synthase is one of the most attractive antibiotic drug targets because its function is essential for cell survival. Additionally, ATP synthase is located on the inner membrane of bacteria which allows drugs to induce apoptosis without penetrating the cell completely.

In 2008, selectivity of BDQ towards mycobacterial ATP synthase was compared with mitochondrial ATP synthase in the presence of 100 nM compound. The IC_{50} values obtained for human and mycobacterial ATP synthase were >200 µM and 0.01 µM, respectively. A high selectivity index of >20,000 for BDQ was calculated, which indicates an unlikeliness to induce target-based toxicity in mammalian cells. Additionally, human SMPs (mitochondria with no outer membrane) showed very low sensitivity for BDQ, with an IC_{50} of >200 µM.[9] Based on these results, BDQ may be considered as the first highly selective ATP synthase inhibitor with the potential to treat a bacterial infection.

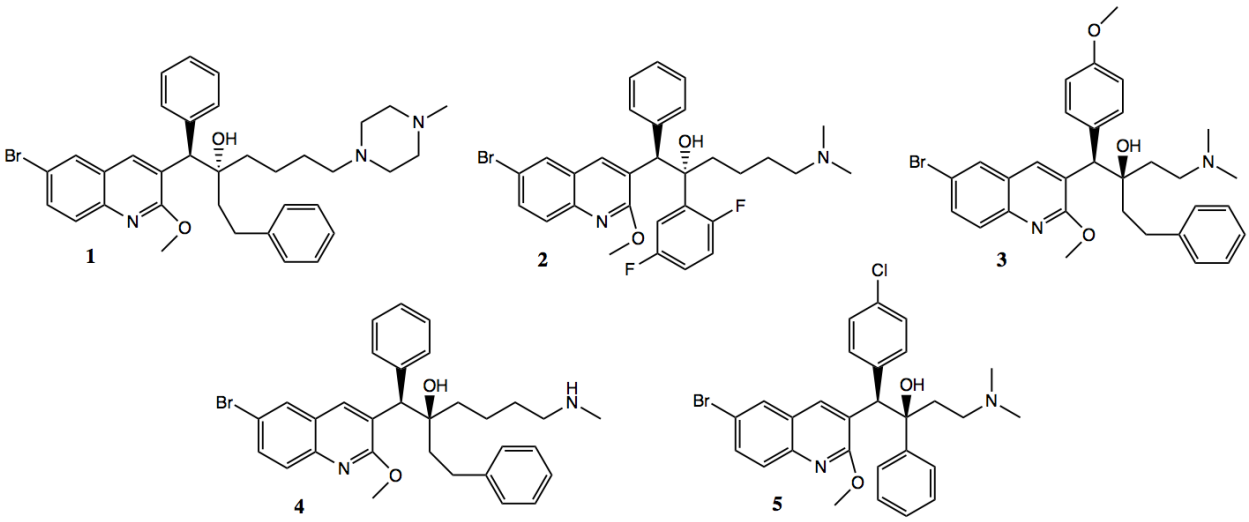

Figure 3. Chemical structures of compounds 1-5 produced by Balemans and co-workers from 2012.[10]

In 2012, key researchers in the field, Guillemont and coworkers, explored the possibilities of BDQ as a broad spectrum drug by testing various synthesized derivatives against Gram-positive and Gram-negative bacteria. Over 700 molecules with novel lateral chains were synthesized and evaluated for antibacterial activity. The five compounds (Figure 3) discussed in the study are representative of having shown activity against key Gram-positive human pathogens. The first three resulted with strong inhibited growth of various Gram-positive bacteria having most success with *Streptococcus pneumoniae* with a MIC value of 0.25 µg/mL. Results with *S. aureus* were not as promising unless at high concentrations. The study also tested against *E. coli* with best IC_{50} values at around 8 µg/mL. The leading compound contained elongated chains of both the dimethylamino and phenyl groups. However, the researchers concluded that the drugs did not have much effect, potentially due to drug efflux mechanisms, less-pronounced metabolic dependency on ATP synthase, and the thick outer membrane of Gram-negative bacteria.[10]

In 2019, the potential of the antibiotic optochin, a semisynthetic derivative of quinine, was explored via a structure-activity relationship study by Wang and coworkers.[11] Their analog **48** (Figure 4) has a MIC that ranges from 8-16 times lower than optochin when tested against the Gram-positive bacteria, *Streptococcus pneumoniae*.

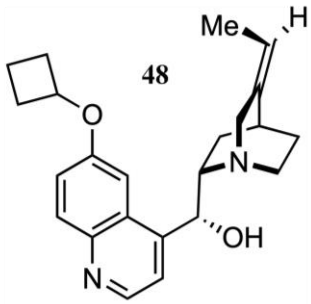

Figure 4. Potent optochin analog **48** prodused by Wang and coworkers.

However, the analog demonstrated no antibacterial activity against the ESKAPE pathogens (i.e. *Enterococcus faecium, Staphylococcus aureus, Klebsiella pneumoniae, Acinetobacter baumannii, Pseudomonas aeruginosa, and Enterobacter species*) nor *E. coli* or *M. tb*. After various biological experiments and molecular modeling studies, they conclude that optochin and its analogs bind within close proximity of the ion binding site on the c-ring of ATP synthase.[11]

In 2015, Priess et. al. addressed the limited understanding of BDQ's precise interactions with the c-ring by performing a biochemical and x-ray crystallography study to provide the amino acid alignment of selected ATP synthase c-

subunits (Figure 5).[7] The size of the drug allows it to make an an extensive amount of van der Waals interactions with a total of nine residues branching from two adjacent subunits, including Gly[62], Leu[63], Glu[65], Ala[66], Ala[67], Tyr[68], Phe[69], Ile[70], and Leu[72]. The functional groups of the dimethylamino chain of BDQ, which penetrates the binding site, form the strongest bonds with Glu[65]. The hydroxyl group interacts with Glu[65] by forming a hydrogen bond with a buried water molecule. The dimethylamino group directly forms an ionic intermolecular hydrogen bond with Glu[65]'s carboxyl group at a distance of 2.5 Å.

Figure 5. Amino acid differences between *M. tb.* H37Rv, *E. coli, H. sapiens,* and *S. aureus.* Amino acids within the ion-binding site region are cyan, and residues that participate in binding are highlighted with navy blue. Amino acids previously shown to cause a BDQ resistance upon mutation have been seen at positions 63, 65, 67 and 70.

BDQ is highly specific towards mycobacterial c-rings due to differing amino acid sequences of F-ATPase across species. For example, the hydrogen bond accepting Asp[32] also plays a critical role with BDQ binding, but is typically replaced with small aliphatic residues in Gram-negative bacteria. This mutation leads to subtle, yet disrupting, changes to the hydrogen bonding network of the binding site. However, the terminal helices of the ATP synthase of *M. tb* (H37Rv) and *E. coli* can be compared and used to make substituent changes on BDQ in order to better target *E. coli.* As stated, amino acids critical to binding are located at positions 32 and 65; therefore, the change from Asp[32] to Ile[32], and Glu[65] to Asp[65], must be taken into account when designing analogs. Considering the potential of bedaquiline as an antibacterial drug seen thus far, the focus here was to synthesize various BDQ analogs in order to target ATP synthase in other Gram-negative bacteria, specifically *Escherichia coli.*

Previous analogous research of BDQ done by He and co-workers in 2016 addressed BDQs difficult stereo-structural complexity, chemical synthesis, and compound optimization.[4] To improve these difficulties, simplified analogs were synthesized to create new, alternative leads. Although analogs synthesized by He 2016 target *M. tb*., the most relevant and promising of those were used as a starting point for this work. In addition, the same study shows analogs with special modification to C2 (Figure 1) with the best MICs (0.43-2.5 µg/mL) having some variation of a benzyl ether.[4]

Studies evaluating bedaquiline derivatives against bacteria other than *M. tb*. are limited, but the advancement in this research topic could increase BDQs potential in becoming a broad spectrum drug and may have an effect on other MDR strains. Since efficient synthesis and mass-production of drugs with novel mechanisms of action for MDR Gram-negative bacteria is greatly needed, this work aims to take the subtle AA sequence changes into consideration in order to develop a series of synthesis efficient BDQ analogs which bind to the F_o c-ring subunit of ATP synthase of the Gram-negative *E. coli*. In this regard, various simplified analogs with a diarylquinoline chemical scaffold are proposed to probe the structure activity relationship of the C2 and C3 positions of BDQ for evaluation against the Gram-negative bacteria, *Escherichia coli* (Scheme 1). Potency of synthesized compounds are tested on replicating *Staphylococcus aureus and Escherichia coli* pathogens. The results presented here demonstrate the potential of these compounds as novel starting points for discovering new antibiotics to combat multidrug resistance.

2. Methods and Experimental

2.1 Cell Death Assay

IC_{50} values of compounds incubated with *Escherichia coli* and *Staphylococcus aureus* cells were determined via a 96 well broth 10 fold dilution assay with compound concentrations varying from 1,000 g/mL to 0.1 ng/mL. Chloramphenicol was used as the positive control. Briefly, 1 µL of compound in DMSO, 89 µL of full strength tryptic soy broth (FS TSB), and 10 µL of the bacterium in FS TSB was added to each well. Assays were incubated for approximately 18 h at 37 ºC and absorbance was read at 590 nm on a Synergy HTX microplate reader.

2.2 ATP-driven H^+ pumping assay

F_1F_o activity was determined from isolated membrane vesicles prepared in a collaborating laboratory from *Escherichia coli* JWP292 carrying plasmid pCMA113. Briefly, 3.2 mL room temperature HMK Buffer (50 mM HEPES-KOH pH 7.5, 2 mM $MgCl_2$, 300 mM KCl), 160 µL ISO membranes (10 mg/mL), and 8 µL 9-amino-6-chloro-2-methoxyacridine (ACMA) were added to a test tube and vortexed. Excitation at 415 nm, emission at 485 nm. Time course was initiated with the addition of 30 µL (25 mM) ATP at 20 s, followed by the addition of 8 µL nigericin at 100 s. The addition of analogs was varied in the concentration of 1 µM - 1 mM. Fluorescence was monitored by an Aminco Bowman Series 2 luminescence spectrometer.

2.3 Chemistry

All reagents and anhydrous solvents were purchased from commercially available sources and were used without further purification. The following solvent abbreviations are used: (Hex) hexane, (EA) ethyl acetate, (DMF) dimethylformamide, and (THF) tetrahydrofuran. All reactions were monitored by TLC. Flash column chromatography was performed with silica gel (mesh size 250). Purity was determined by LCMS and NMR spectroscopy. LCMS spectral data were obtained using CH_3OH/H_2O with 1% acetic acid on Shimadzu LCMS-2020. ^1H and ^{13}C NMR spectral data were obtained using $CDCl_3$ as the solvent on a Varian Gemini 2000 and Oxford Instruments 400M Hz superconducting magnet using TMS as internal standard. Chemical shifts (d) are reported in ppm and coupling constants (J) are given in hertz (Hz). The following multiplicity abbreviations are used: (s) singlet, (d) doublet, (t) triplet, (q) quartet, (m) multiplet, and (br) broad. See the Supporting Information for detailed characterization of all intermediates and final compounds.

2.4 General Procedure for Electrophilic Aromatic Substitution (EAS) Reactions[4]

A 100 mL, oven-dried, 1-neck round bottom flask (RBF) was fitted with a stir bar and condenser and placed under an inert Ar atmosphere. The RBF was submerged in an oil bath that was warmed to 90 ºC and monitored with a thermometer. 2-chloroquinoline-3-carbaldehyde (200 mg, 1.0 mmol) and the chosen alcohol (~200 mg, 1.26 mmol) were then added to the flask. A 30 mL plastic syringe was then used to add 12 mL DMF (0.085 M) while stirring to make a darkening yellow solution. Finally, Cs_2CO_3 (500 mg, 1.53 mmol) was added. The mixture was allowed to react for 24 h. TLC was performed using 50:50 Hex:EA.

The solution was then treated with 20 mL of water and extracted with methylene chloride (CH_2Cl_2) (3x20 mL). The combined organic layers were dried with $NaSO_4$, filtered and concentrated under pressure. The crude product was then purified by flash column chromatography (SiO_2, 97:3 Hex:EA) to afford a cream or yellow colored solid.

2.5 General Procedure for Horner–Wadsworth–Emmons (HWE) Olefination[12]

An oven-dried, 1-neck round bottom flask (RBF) was fitted with a stir bar and placed under an inert Ar atmosphere. The RBF was submerged in an ice bath that was cooled to 0 ºC. Triethyl phosphonoacetate (1.5 mL, 3.07 mmol) and sodium hydride (~200 mg, 2.84 mmol) were then added to the flask. A 30 mL plastic syringe was then used to add in 15 mL of THF (0.17 M) while stirring to make a milky white solution. The mixture was removed from the ice bath and allowed to warm to room temperature. After 30 minutes the reaction was recooled to 0 ºC, and a substituted quinoline carbaldehyde was added (800 mg, 2.56 mmol) was added as a solution in 3 mL THF. The mixture was allowed to warm to room temperature and react for 20 h. TLC was performed using 50:50 Hex:EA.

The solution was then treated with 20 mL of saturated ammonium chloride and extracted with diethyl ether (3x20 mL). The combined organic layers were washed with water (2x15 mL), dried with $MgSO_4$, filtered and concentrated under pressure. The resulting residue was then purified by flash column chromatography (SiO_2, 97:3 Hex:EA) to afford a white solid.

2.6 General Procedure for the Reduction of Acrylates[12]

DIBAL-H 20 wt% solution in toluene (1 mL, 2.52 mmol) was added slowly to the chosen acrylated analog (1.31 mmol) in CH_2Cl_2 (20 mL) at 0 °C. The mixture was removed from the ice bath and allowed to react at room

temperature for 2 h. The reaction was then treated with 20 mL saturated aqueous Rochelle's salt at 0 °C, and the resulting suspension was stirred vigorously for 4 h. The reaction mixture was filtered and the two layers separated. The aqueous layer was further extracted with CH^2Cl_2 (3x20 mL). The combined organic layers were dried with Na_2SO_4 and concentrated under reduced pressure. The resulting residue was then purified by flash column chromatography (SiO_2, 97:3 Hex:EA).

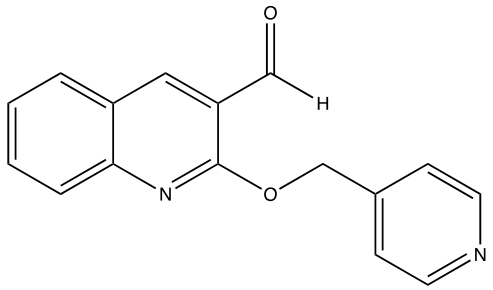

2-(pyridin-4-ylmethoxy)quinoline-3-carbaldehyde (6a): The general EAS procedure was followed using 2-chloroquinoline-3-carbaldehyde (200 mg, 1.0 mmol) and 4-pyridinemethanol (144 mg, 1.26 mmol). Flash chromatography (SiO2, 2 × 10 cm, 0-8% EtOAc/hexanes gradient elution) afforded analog **6a** as a yellow solid (75 mg, 38%). [M+1] expected 265, observed 265. **^{1}H NMR:** ($CDCl_3$-d_l, 400M Hz) δ 10.6 (s, 1H), 8.67 (s, 1H), 8.64 (d, 2H), 7.88-7.45 (7H), 5.71 (s, 2H), see supporting information.

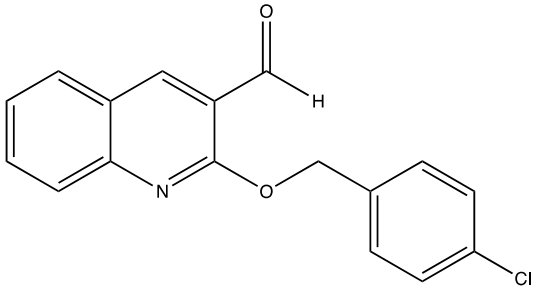

2-((4-chlorobenzyl)oxy)quinoline-3-carbaldehyde (7a): The general EAS procedure was repeated using 2-chloroquinoline-3-carbaldehyde (200 mg, 1.0 mmol) and (4-chlorophenyl)methanol (187 mg, 1.26 mmol). Flash chromatography (SiO2, 2 × 10 cm, 0-8% EtOAc/hexanes gradient elution) afforded analog **7a** as a yellow solid (5 mg, 2%). [M+1] expected 298, observed 298. **^{1}H NMR:** ($CDCl_3$-d_l, 400M Hz) δ 10.5 (s, 1H), 8.64 (s, 1H), 7.88 (m, 2H), 7.77 (t, 1H), 7.50 (m, 3H), 7.38 (m, 2H), 7.37 (m, 1H), 5.65 (s, 2H) see supporting information.

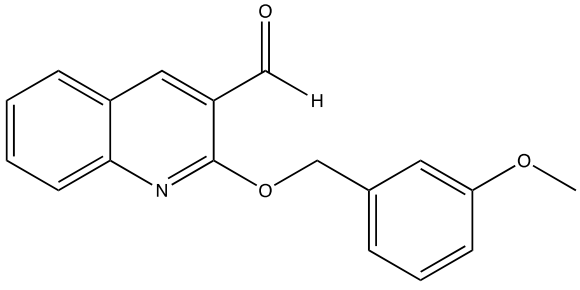

2-((3-methoxybenzyl)oxy)quinoline-3-carbaldehyde (8a): The general EAS procedure was repeated using 2-chloroquinoline-3-carbaldehyde (200 mg, 1.0 mmol) and (3-methoxyphenyl)methanol (182 mg, 1.26 mmol). Flash chromatography (SiO2, 2 × 10 cm, 0-8% EtOAc/hexanes gradient elution) afforded analog **8a** as a yellow solid (5 mg, <5%). [M+1] expected 294, observed 294. **^{1}H NMR:** ($CDCl_3$-d_l, 400M Hz) δ 10.6 (s, 1H), 8.64 (s, 1H), 8.11-6.92 (9H), 5.13 (s, 2H), 3.71 (s, 3H), see supporting information.

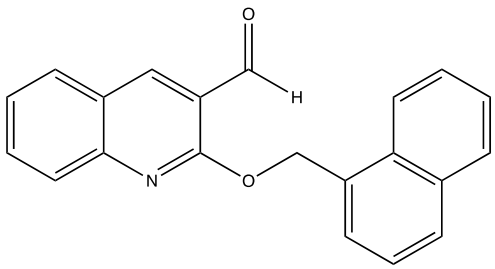

2-(naphthalen-1-ylmethoxy)quinoline-3-carbaldehyde (9a): The general EAS procedure was repeated using 2-chloroquinoline-3-carbaldehyde (2 g, 1.0 mmol) and 1-naphthalenemethanol (6 g, 2 mmol). Flash chromatography (SiO2, 3 × 10 cm, 0-3% EtOAc/hexanes gradient elution) afforded analog **9a** as a white solid (800 mg, 25%). [M+1] expected 314, observed 314. **^{1}H NMR:** ($CDCl_3$-d_I, 400M Hz) δ 10.4 (s, 1H), 8.64 (s, 1H), 8.11-7.45 (m, 12H), 6.13 (s, 2H), see supporting information.

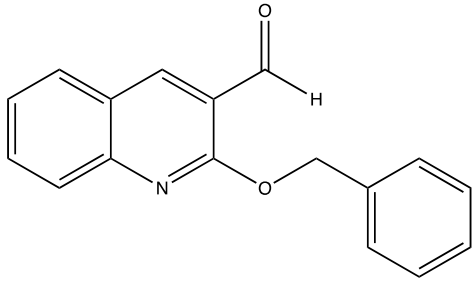

2-(benzyloxy)quinoline-3-carbaldehyde (10a): The general EAS procedure was repeated using 2-hydroxyquinoline-3-carbaldehyde (200 mg, 1.0 mmol) and phenylmethanol (142 mg, 1.26 mmol). Flash chromatography (SiO2, 2 × 10 cm, 0-3% EtOAc/hexanes gradient elution) afforded analog **10a** as dark oil (5 mg, 2%). [M-1] expected 262, observed 262. **^{1}H NMR:** ($CDCl_3$-d_I, 400M Hz) δ 10.5 (s, 1H), 8.46 (s, 1H), 7.76 (d, 1H), 7.59 (m, 2H), 7.44 (d, 1H), 7.38-7.25, (m, 5H), 5.58 (s, 2H), see supporting information.

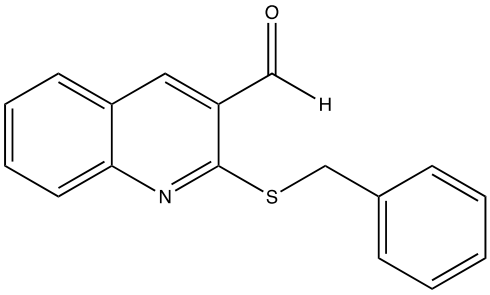

2-(benzylmercaptan)quinoline-3-carbaldehyde (11a): The general EAS procedure was repeated using 2-hydroxyquinoline-3-carbaldehyde (200 mg, 1.0 mmol) and benzyl mercaptan (2 mL, 194 mg, 1.5 mmol). Flash chromatography (SiO2, 2 × 10 cm, 0-5% EtOAc/hexanes gradient elution) afforded analog **11a** as a yellow solid (164 mg, 38%). [M+1] expected 280, observed 280. **^{1}H NMR:** ($CDCl_3$-d_I, 400M Hz) δ 10.2 (s, 1H), 8.44 (s, 1H), 7.90 (d, 1H), 7.75 (d, 1H), 7.67 (t, 1H), 7.45 (m, 3H), 4.95 (t, 1H), 4.54 (1, 2H), 4.23 (s, 1H), 3.84 (s, 2H), 3.39 (s, 2H) see supporting information.

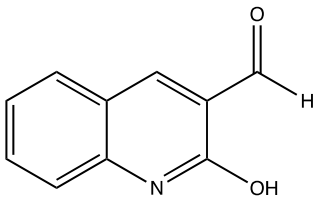

2-hydroxyquinoline-3-carbaldehyde (12a): The general EAS procedure was repeated using 2-chloroquinoline-3-carbaldehyde (200 mg, 1.0 mmol) and sodium hydroxide (53 mg, 1.26 mmol). Flash chromatography (SiO2, 2 × 10 cm, 5-30% EtOAc/hexanes gradient elution) afforded analog **12a** as a white solid (7 mg, 4%). [M+1] expected 174, observed 174. **^{1}H NMR:** ($CDCl_3$-d_l, 400M Hz) δ 10.2 (s, 1H), 8.46 (s, 1H), 7.78 (t, 2H), 7.69 (t, 1H), 7.31 (t, 1H), see supporting information.

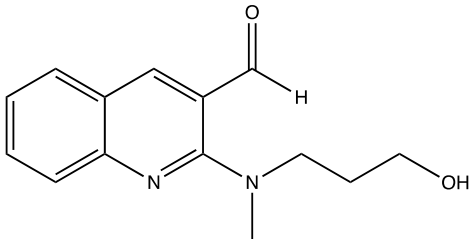

2-((3-hydroxypropyl)(methyl)amino)quinoline-3-carbaldehyde (13a): The general EAS procedure was repeated using 2-chloroquinoline-3-carbaldehyde (200 mg, 1.0 mmol) and N,N-dimethylaminopropanol (136 mg, 1.26 mmol) under thermodynamic conditions. Flash chromatography (SiO2, 2 × 10 cm, 5-20% EtOAc/hexanes gradient elution) afforded analog **13a** as a dark oil (6 mg, 2%). [M-1] expected 257, observed 257. **^{1}H NMR:** ($CDCl_3$-d_l, 400M Hz) δ 10.1 (s, 1H), 8.45 (s, 1H), 7.74 (d, 1H), 7.67 (t, 2H), 7.30 (m, 1H), 3.94 (t, 2H), 3.57 (t, 2H), 3.08 (s, 3H), 1.97 (m, 2H) see supporting information.

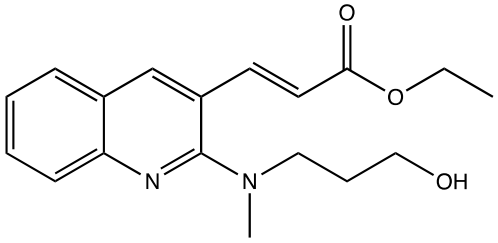

ethyl (*E*)-3-(2-((3-hydroxypropyl)(methyl)amino)quinolin-3-yl)acrylate (13b): The general HWE procedure was followed using triethyl phosphonoacetate (220 mg, 1.2 mol) and sodium hydride (22 mg, 1.1 mol) dissolved in 15.5 mL of dry THF. An addition funnel was used to gradually add analog **13a** (200 mg, 1 mol) and after 20 minutes the solution was allowed to warm to room temperature and react for 24 hours. The resulting residue was purified by flash column chromatography (SiO_2, 2 × 10 cm, 0-10% EtOAc/hexanes gradient elution) to afford analog **13b** as a yellow solid (3 mg, <1%). [M+1] expected 315, observed 315.

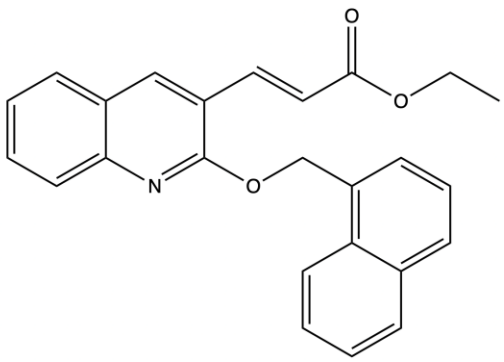

ethyl (*E*)-3-(2-(naphthanol)quinolin-3-yl)acrylate (9b): The general procedure for HWE olefination was followed using analog **9a** (800 mg, 0.26 mmol), triethyl phosphonoacetate (1.5 mL, 687 mg, 0.31 mmol), and sodium hydride (112 mg, 0.28 mmol) in 25 mL THF (0.10 M). Flash chromatography (SiO2, 2 × 10 cm, 0-5% EtOAc/hexanes gradient elution) afforded analog **9b** as a white solid (300 mg, 82%). [M+1] expected 384, observed 384. **^{1}H NMR:** ($CDCl_3$-d_l, 400M Hz) δ 8.21 (d, 2H), 7.98 (m, 4H), 7.75 (t, 2H), 7.67 (t, 2H), 7.51 (m, 3H), 7.42 (t, 1H), 6.12 (s, 2H), 4.20 (q, 2H), 1.56 (s, 4H), 1.28 (t, 3H) see supporting information.

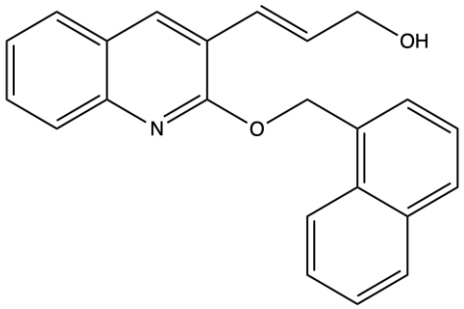

(*E*)-3-(2-methyl-3-quinolyl(2-naphthanol)-2-propenol (9c): The general procedure for acrylate reduction was followed using analog **9b:** The general procedure for the reduction of acrylates was followed using analog **9b** (300 mg, 0.78 mmol), DIBAL-H (2.43 mL, 4.02 mmol) in CH_2Cl_2 (20 mL). Flash chromatography (SiO2, 2 × 10 cm, 0-5% EtOAc/hexanes gradient elution) afforded analog **9b** as a white solid (262 mg, 87%). [M+1] expected 342, observed 342. **^{1}H NMR:** ($CDCl_3$-d_l, 400M Hz) δ 8.16 (d, 1H), 8.04 (s, 1H), 7.88 (m, 3H), 7.71 (d, 2H), 7.61 (t, 1H), 7.51 (m, 3H), 7.38 (t, 1H), 6.80 (d, 1H), 6.51 (dt, 1H), 6.03 (s, 2H), 4.21 (d, 2H) see supporting information.

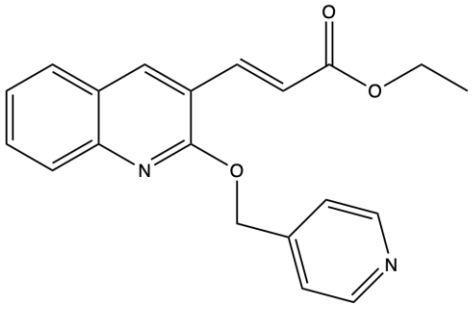

ethyl (*E*)-3-(2-(pyridin-4-ylmethoxy)quinolin-3-yl)acrylate (6b): The general procedure for HWE olefination was followed using analog **6a** (70 mg, 0.26 mmol), triethyl phosphonoacetate (71 mg, 0.32 mmol), and sodium hydride (10 mg, 0.42 mmol). Flash chromatography (SiO2, 2 × 10 cm, 5-20% EtOAc/hexanes gradient elution) afforded analog **6b** as a yellow solid (4 mg, <1%). [M+1] expected 335, observed 335.

3. Results and Discussion

3.1 Synthesis of simplified bedaquiline analogs

The structure of bedaquiline contains a core quinoline moiety along with two adjacent chiral carbons bonded to three aryl rings and a dimethylamino group (Figure 1). Based on structure and antitubercular activity relationship findings made by Preiss et. al and He et. al., the contribution of each fragment was determined. Some fragments, such as the quinoline and dimethylamino groups, are necessary to maintain its activity, whereas other groups such as the bromo and hydroxyl groups are less critical. Based on this information initial stages of the project have been set to focus on modification of the methoxy on C2 (Figure 1) by adding more non-polar groups such as substituted benzenes with the hope of increasing sterics. The general synthesis of the first series of analogs is depicted in Scheme 1, which consists of an electrophilic aromatic substitution reaction with a commercially purchased chlorinated quinoline and a substituted benzyl alcohol or benzyl mercaptan. The mercaptan moiety is included to confirm the necessity of an oxygen at that position.

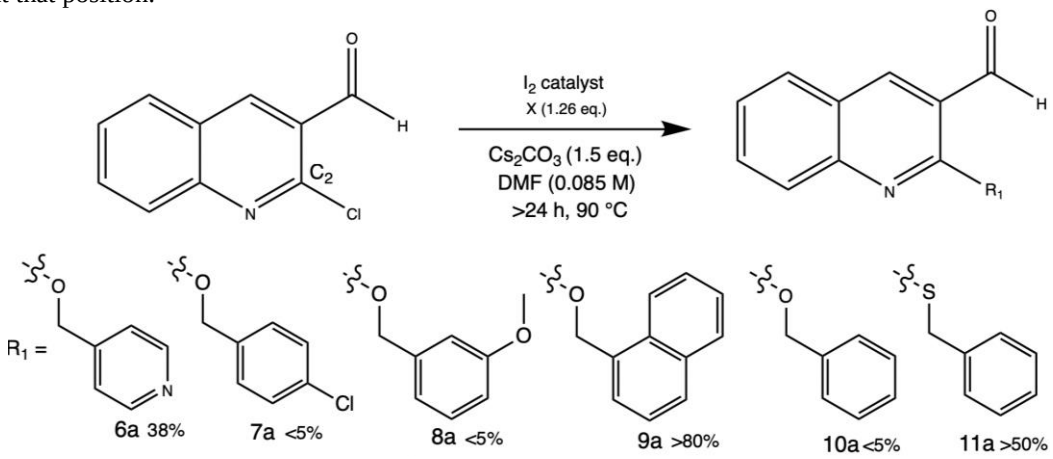

Scheme 1. Synthesis of various simplified BDQ analogs.

First attempts at synthesis of the first series of analogs resulted with extremely low yields ranging from 1%-10%. It was assumed that this was due to a combination of the poor reactibility of such sterically large nucleophiles with the starting material or poor execution of purification via column chromatography. Therefore, reaction conditions were optimized by replacing K_2CO_3 with a stronger, and more soluble base, such as Cs_2CO_3, the temperature was increased by 10 ºC, and reaction time was extended. The polarity of the mobile phase for column chromatography was decreased to 97:3 hexanes:ethyl acetate. Analog **9a** was expected to have most activity against both Gram-positive and Gram-negative pathogens until more hydrogen bond accepting substituents are added because of naphthalene's steric bulk.

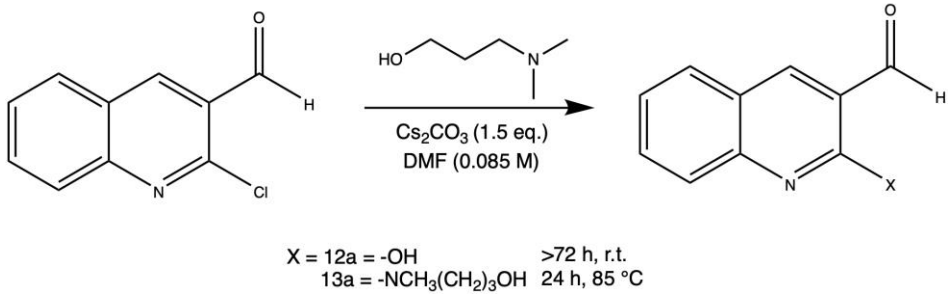

Scheme 2. General synthesis for analogs 12a-13a including kinetic and thermodynamic reaction conditions.

A structurally different analog, containing a N,N-dimethylaminopropanol chain on C2 was also attempted to compare potential activity with the same group on C3 (Scheme 2). Various combinations of kinetic and thermodynamic reaction

conditions resulted in the formation of potentially four different compounds (Figure 6). Under kinetic conditions, the nucleophile will react on itself and cyclize, cleaving the alcohol and allowing it to react with the chloroquinoline starting material, affording compound **12a**. Interestingly, in addition to this product, mass spectrometry analysis indicates that compound **13d** was also synthesized. Under thermodynamic conditions, the nitrogen of the dimethylamino chain is able to attack the electrophilic C2 of the starting material, affording compound **13a**. On rare occasion, mass spectrometry analysis has indicated that the initial desired compound, **13e**, was synthesized.

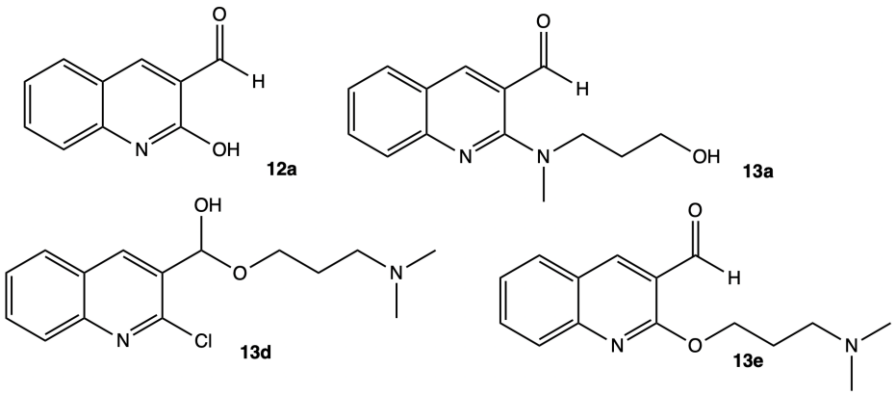

Figure 6. 2D chemical structures of potential reaction products from Scheme 2.

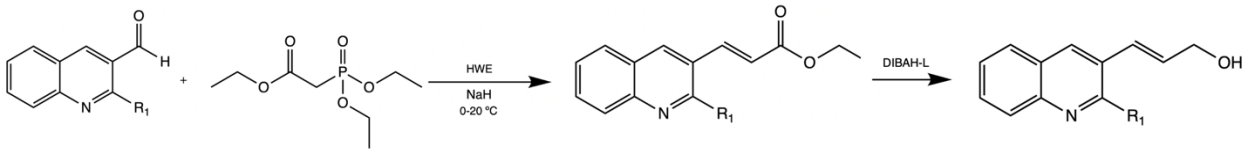

Scheme 3. General synthesis for next set of analogs which combine both upper and lower modifications.

The next series of analogs combines modifications made on both C2 and C3 using Scheme 3, which first reacts one of the analogs from the first series (**6a**-**13a**) with triethyl phosphonoacetate in a Horner Wadsworth Emmons Wittig reaction. The intermediate is then reduced with DIBAL-H.

3.2 Evaluation of antibacterial activity of synthesized analogs

Each analog was tested for antibacterial activity using an in-house antibacterial assay against the Gram-positive, *Staphylococcus aureus*, and Gram-negative, *Escherichia coli* (Table 1). A couple issues faced was the insolubility of some analogs in dimethylsulfoxide (DMSO) and their darkness in color. This lead to inaccurate IC_{50} values which is why results are listed in terms of active range in µg/mL. Most compounds had some degree of activity towards *S. aureus*, but **9a**, **12a**, and **13a** were the only analogs to have observed activity against both pathogens. It is assumed that compound **12a** has most activity (10-1000 µg/mL) because of a weak hydrogen bond that is formed between the hydroxyl and residue 65 via a water molecule. These results are promising considering these are simplified molecules when compared to the more complex structure of BDQ.

Table 1. Antibacterial activity of tested compounds from the first series of analogs is shown in terms of range. "N/A" represents no activity was observed for that pathogen.

Compound	R_1	*S. aureus* activity (µg/mL)	*E. coli* activity (µg/mL)
6a	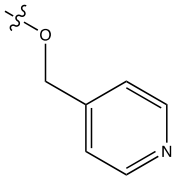	100-1000	N/A
7a	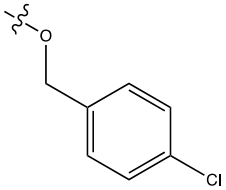	1000	N/A
8a	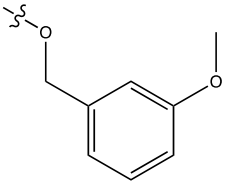	100-1000	N/A
9a	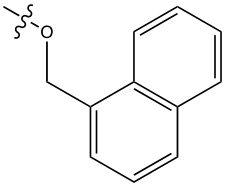	10-1000	1000
11a	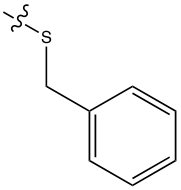	N/A	N/A
12a		10-1000	100-1000
13a	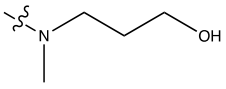	100-1000	100-1000

Table 2. Antibacterial activity of tested compounds from the second series of analogs and their intermediates is shown in terms of range. “N/A” represents no activity was observed for that pathogen.

Compound	Structure	*S. aureus* activity (µg/mL)	*E. coli* activity (µg/mL)
6b	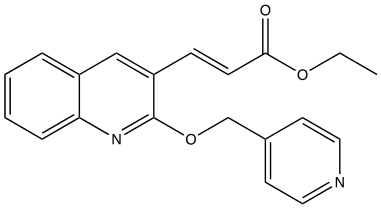	N/A	N/A
13b	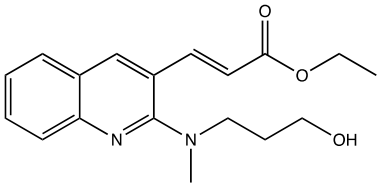	N/A	N/A
9b	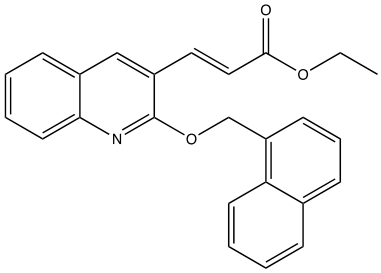	N/A	N/A
9c	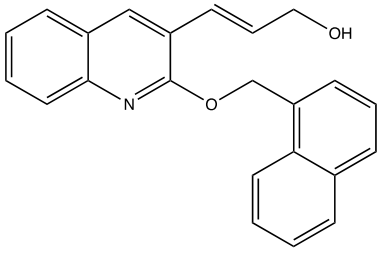	N/A	1000

After evaluating the compounds of Table 2, the most consistent result was analog **9c**, which surprisingly only showed activity at 1000 µg/mL for *E. coli*. This suggests that **9c** is potentially selective for *E. coli.* If **9c** is interacting with the ion binding site, it would be a weak hydrogen bond between the hydroxyl of the chain on C3 and residue 65.

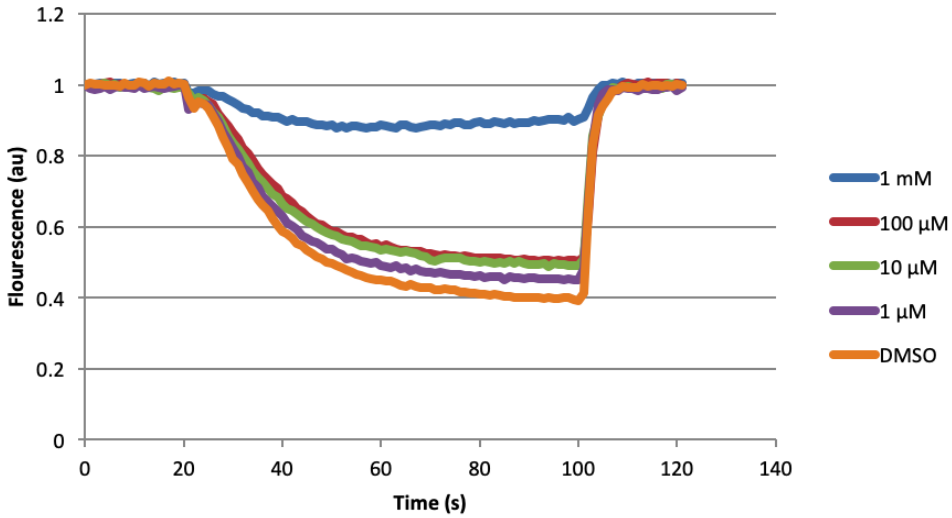

Figure 7. BDQ ATP-driven H^+ pumping assay done by group member, Alex Hanamean, used to establish a negative control for future analogs. All concentrations and reduced activity of F-ATPase is consistent except for 100 nM and 1 mM, which are expected to have reduction in activity.

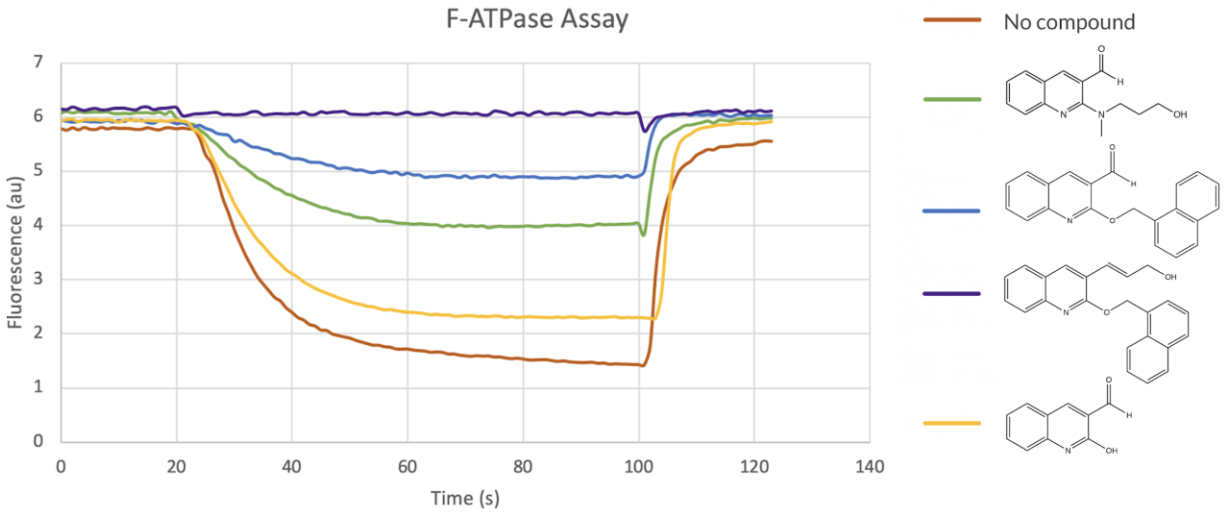

Figure 8. BDQ ATP-driven H^+ pumping assay evaluating selected analog's ability to stall rotor motion of the ATPase c-ring in *Escherichia coli*. The following analogs are evaluated at 1 mM: 13a (green), 9a (blue), 9c (purple), 12a (yellow). Wild type (WT), with no compound, added is represented in red.

The fluorescence-based ATP-driven proton pumping assay is activated by the addition of ATP which starts to pump protons into the enclosed membrane vesicle. The fluorescent molecule, ACMA, also enters the vesicle and becomes protonated, rendering the dye confined within the vesicle and incapable of emitting a fluorescence reading, as seen with the quenching of fluorescence for WT in Figure 7 and 8. Fluorescence is restored once the potassium ionophore, nigericin, is added to promote a K^+/H^+ exchange across the membrane and diffuse any trapped protons.[13] At a concentration of 1 mM, analogs **9a** and **9c**, with the naphthalene substituent, demonstrated best activity with **9c** having the most stable fluorescence reading and outcompetes BDQ. Surprisingly, although analog **12a** showed promising activity for *E. coli* in the cell death assay, very little inhibition activity is seen here (Figure 8). The moderate activity seen for analog **13a**, which gradually quenches fluorescence to 4 au, implies that further structural elaboration is needed. Taken together, the results from both biological assays point towards the promising potential of analog **9c** as a selective compound that targets the c-ring of ATP synthase in *Escherichia coli*.

4. Conclusion

The rising epidemic of drug-resistant bacteria calls for the advances and approaches to antibiotics. Gram-negative bacteria is particularly difficult to penetrate due to its thick outer membrane and therefore has had little advances compared to other bacteria. The novel drug Bedaquiline (BDQ) targets the F-ATP synthase of *Mycobacterium tuberculosis* (*M. tb.*) and stops ATP production and hydrolysis effectively killing the cell. However, it is specific to the amino acid sequencing of *M. tb.* at positions D32, E65, and A67. In the Gram-negative bacteria *Escherichia coli* (*E. coli*), these residues are changed to I32, D65, and I67. Taking into consideration the residue changes and chemical properties of the Gram-negative protective layers, analogs of BDQ can be synthesized to target *E. coli*. The majority of presented analogs (**6a-13a**) have been synthesized and tested for antibacterial activity against both Gram-positive and Gram-negative bacteria using an antibacterial assay. Three of these base analogs, one with a naphthalene substituent, another with a hydroxy, and the other with a N-dimethylaminopropanol, have shown activity toward both *E. coli* and *Staphylococcus aureus* within the 10-1000 µg/mL range. After further elaboration on the base analogs, compound **9c** was discovered to have selective activity against *E. coli* and almost completely terminates c-ring rotation. The results presented here demonstrate the potential of these compounds as novel starting points for discovering new antibiotics to combat multidrug resistance.

5. Supporting Information

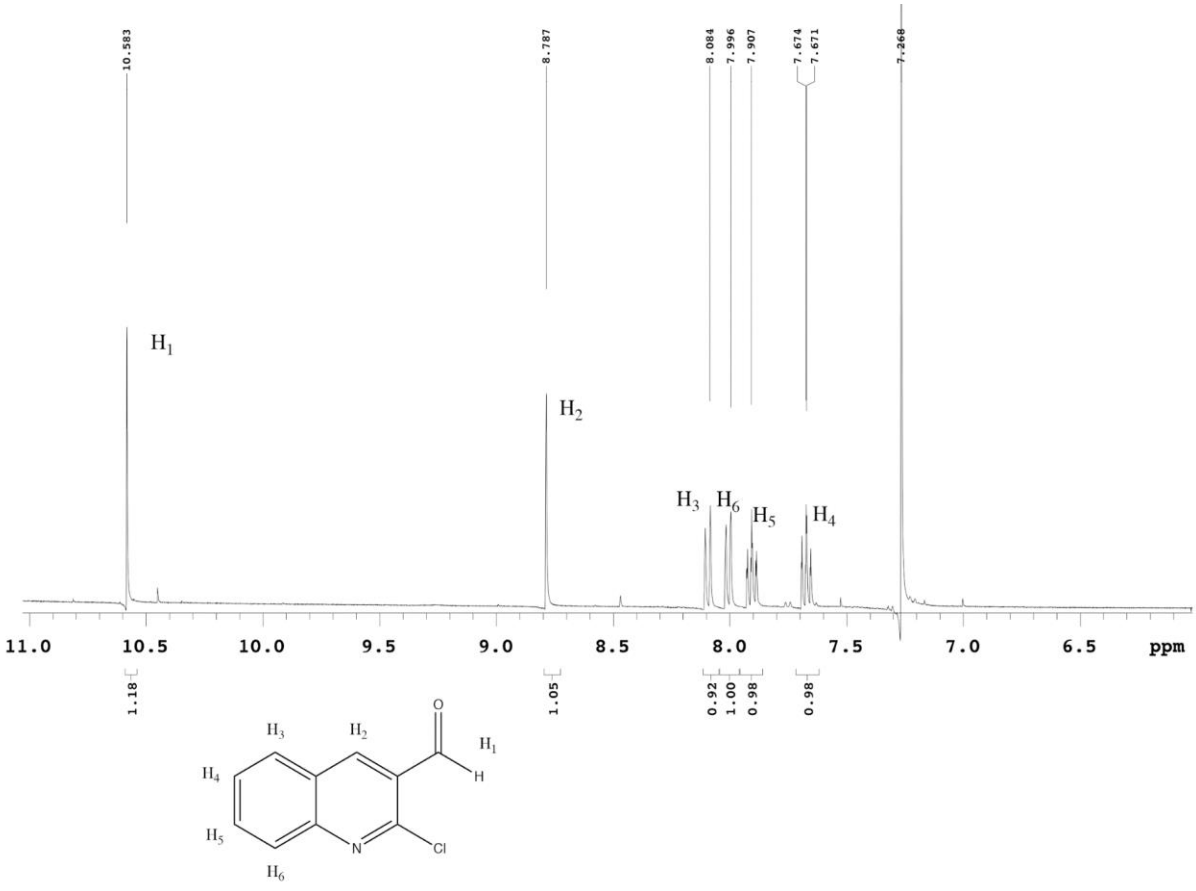

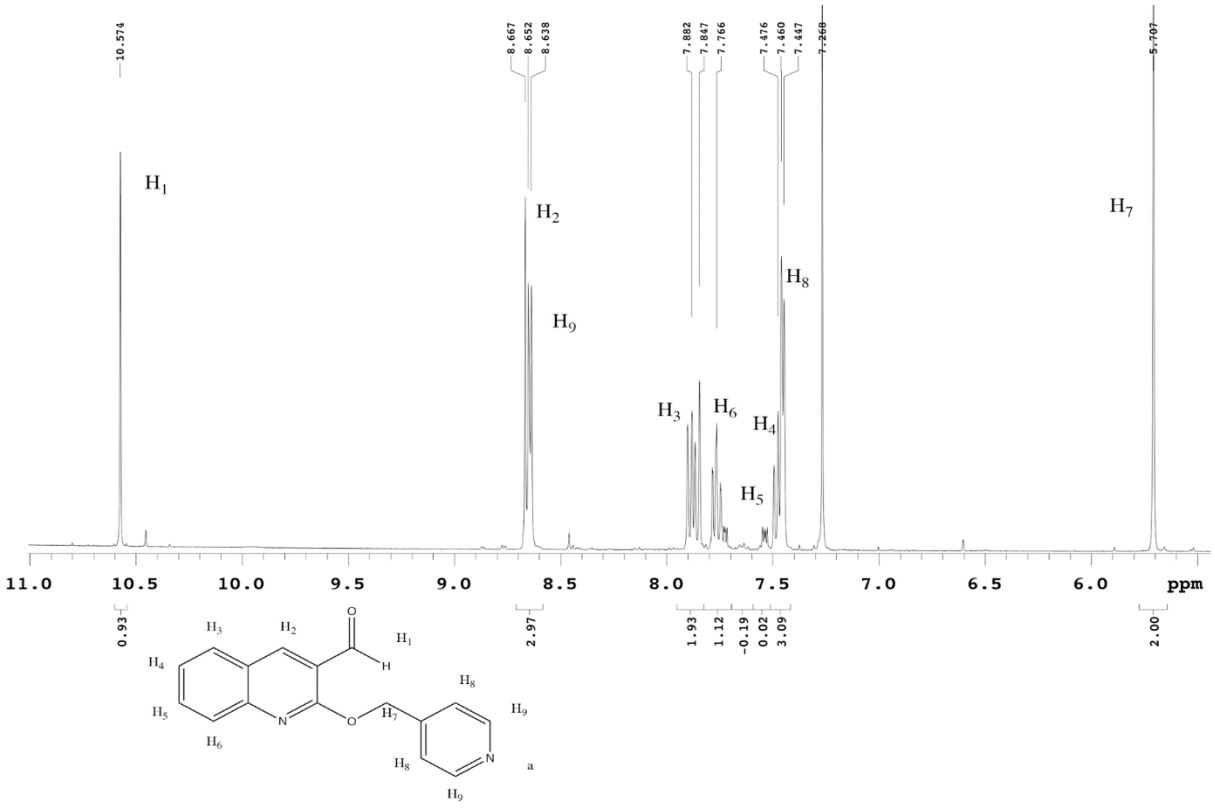

a

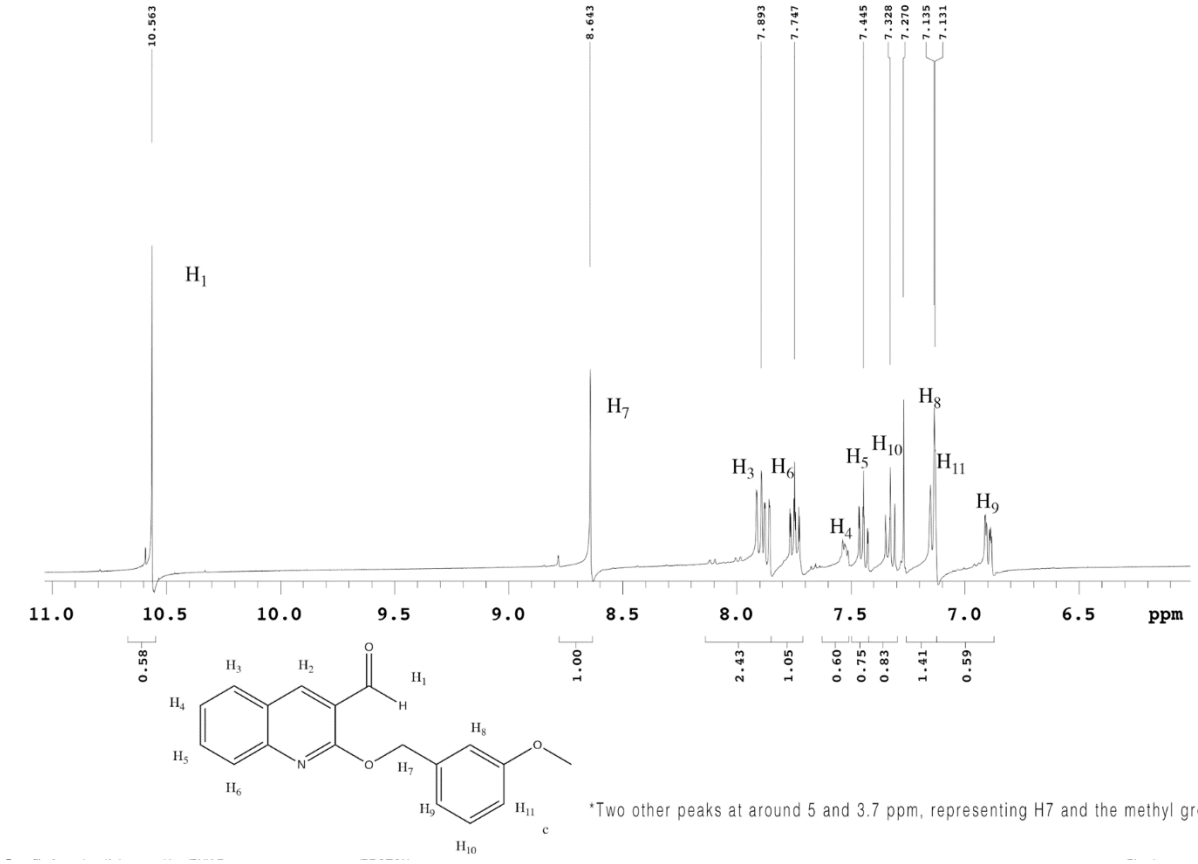

c

*Two other peaks at around 5 and 3.7 ppm, representing H7 and the methyl group.

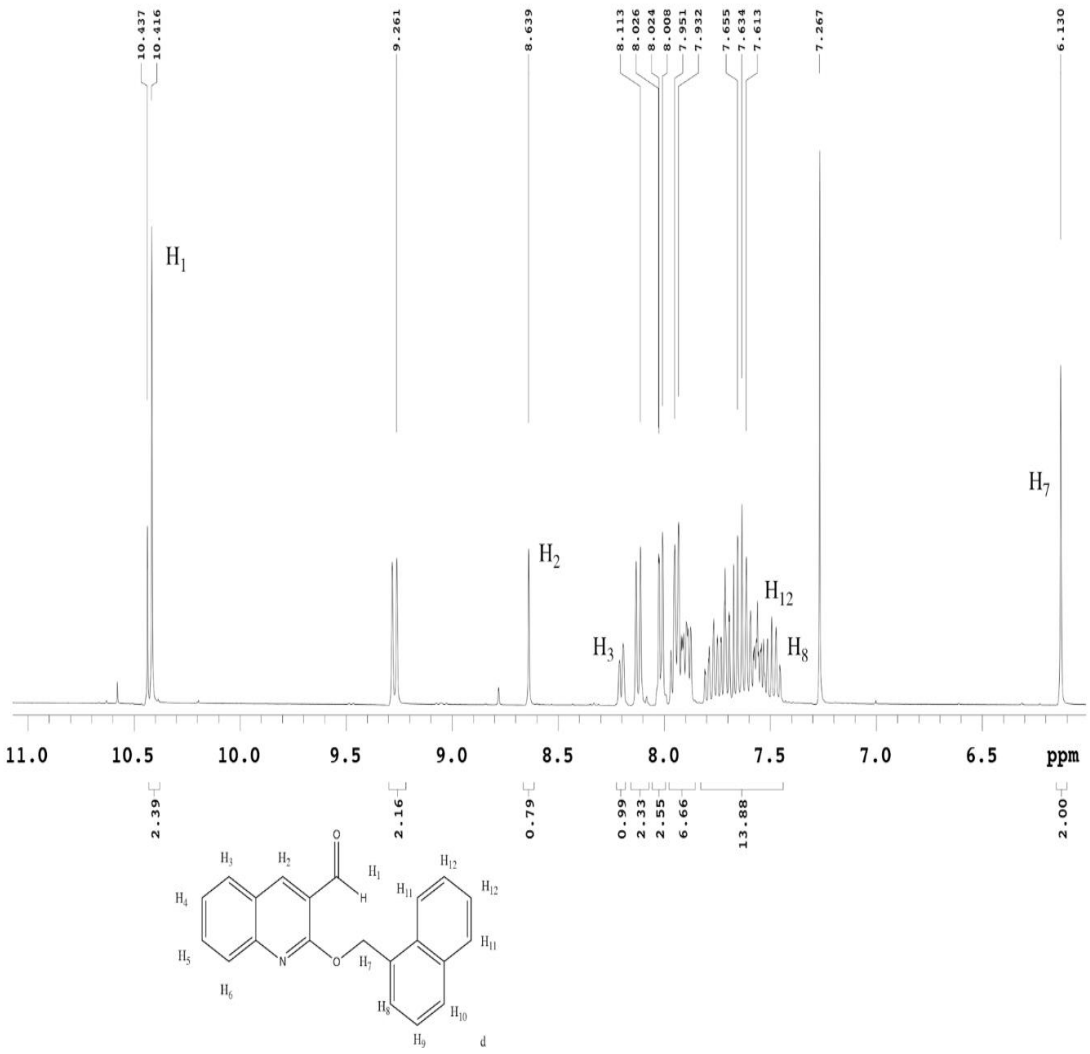
10.437
10.416
9.261
8.639
8.113
8.026
8.024
8.008
7.951
7.932
7.655
7.634
7.613
7.267
6.130
H1
H2
H3
H12
H8
H7
11.0
10.5
10.0
9.5
9.0
8.5
8.0
7.5
7.0
6.5
ppm
2.39
2.16
0.79
0.99
2.33
2.55
6.66
13.88
2.00
O
N
O
H1
H2
H3
H4
H5
H6
H7
H8
H9
H10
H11
H12
d

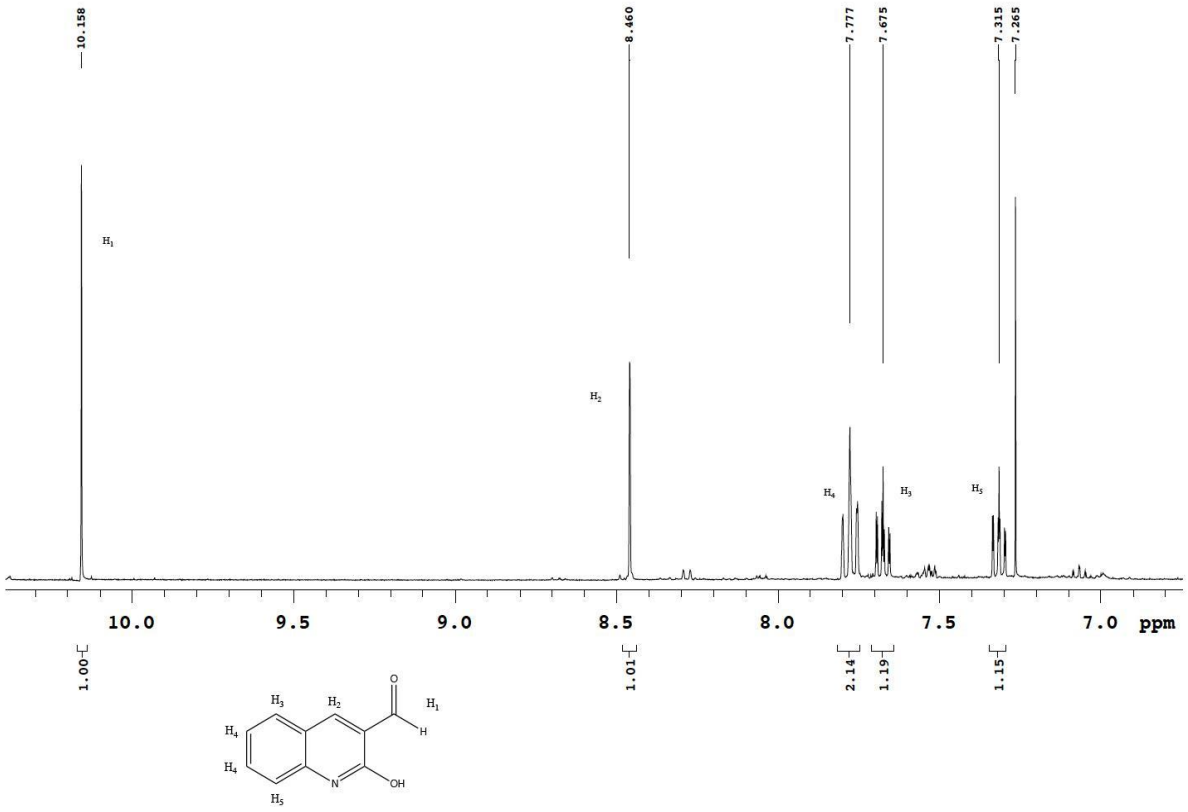
10.158
8.460
7.777
7.675
7.315
7.265
H1
H2
H4
H3
H5
10.0
9.5
9.0
8.5
8.0
7.5
7.0
ppm
1.00
1.01
2.14
1.19
1.15
O
H
OH
N

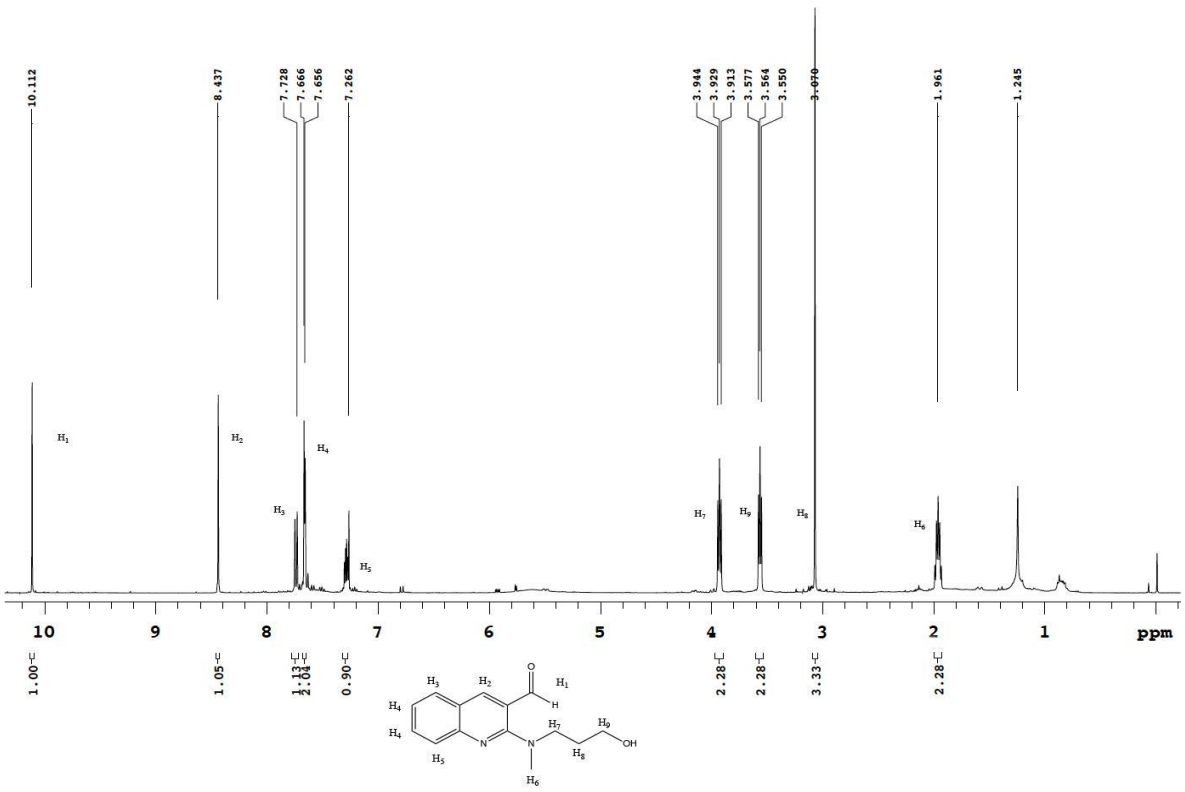
10.112
8.437
7.728
7.666
7.656
7.262
3.944
3.929
3.913
3.577
3.564
3.550
3.070
1.961
1.245
H1
H2
H3
H4
H5
H7
H9
H8
H6
10
9
8
7
6
5
4
3
2
1
ppm
1.00
1.05
1.13
2.04
0.90
2.28
2.28
3.33
2.28
O
H
OH
N

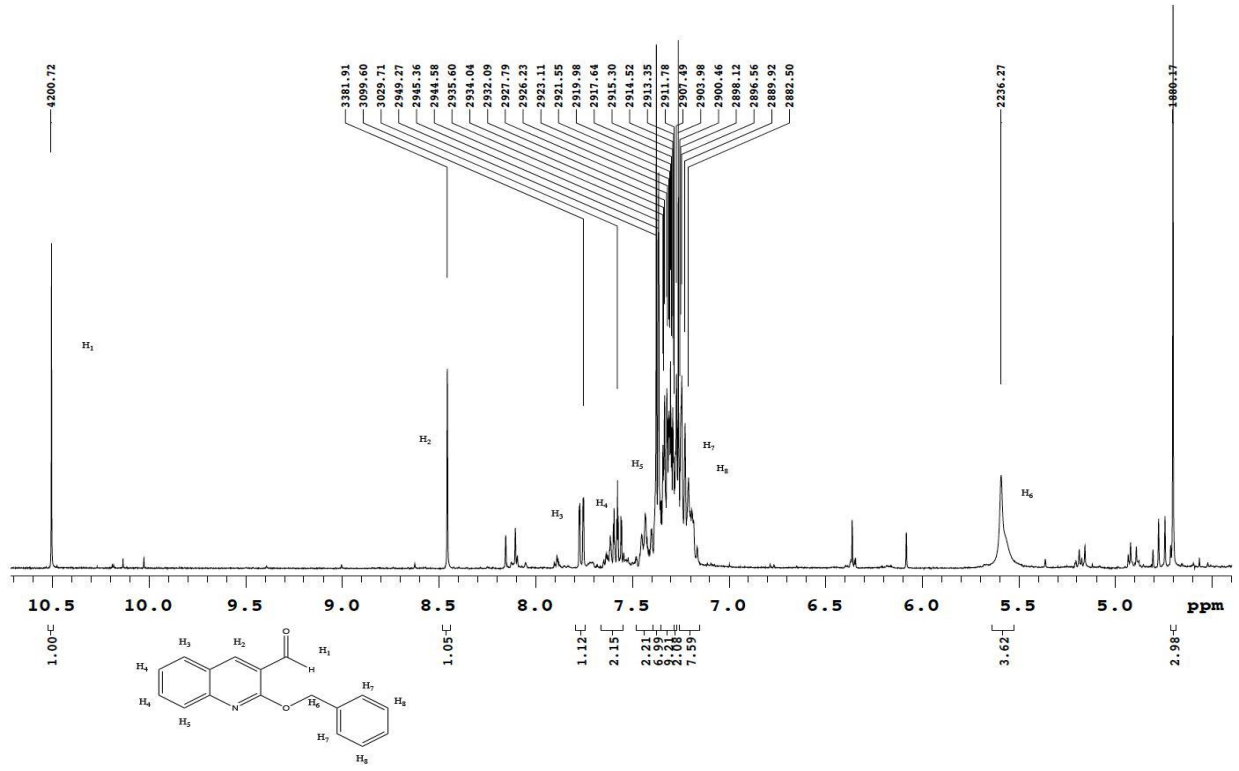
4200.72
3381.91
3099.60
3029.71
2949.27
2945.36
2944.58
2935.60
2934.04
2932.09
2927.79
2926.23
2923.11
2921.55
2919.98
2917.64
2915.30
2914.52
2913.35
2911.78
2907.49
2903.98
2900.46
2898.12
2896.56
2889.92
2882.50
2236.27
1000.17
10.5
10.0
9.5
9.0
8.5
8.0
7.5
7.0
6.5
6.0
5.5
5.0
ppm
1.00
1.05
1.12
2.15
3.62
2.98

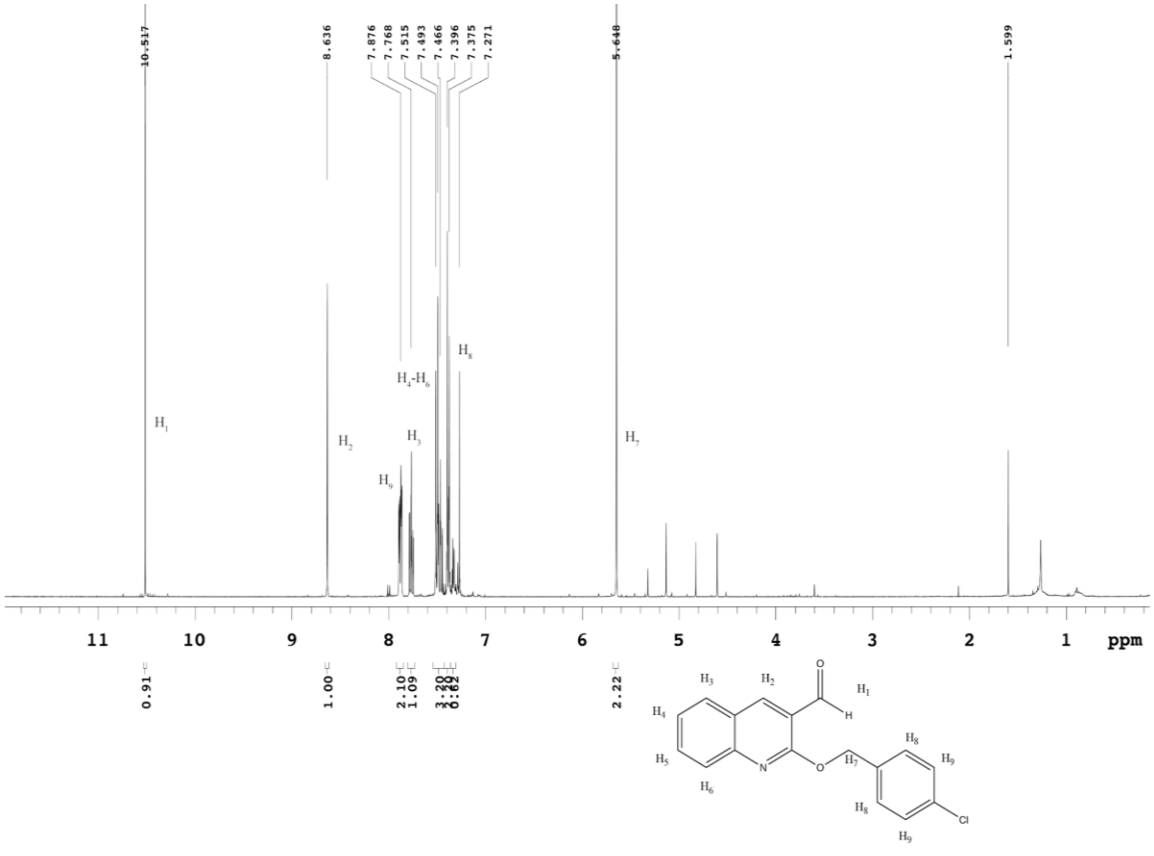
10.517
8.636
7.876
7.768
7.515
7.493
7.466
7.396
7.375
7.271
5.640
1.599
11
10
9
8
7
6
5
4
3
2
1
ppm
0.91
1.00
2.10
1.09
2.22

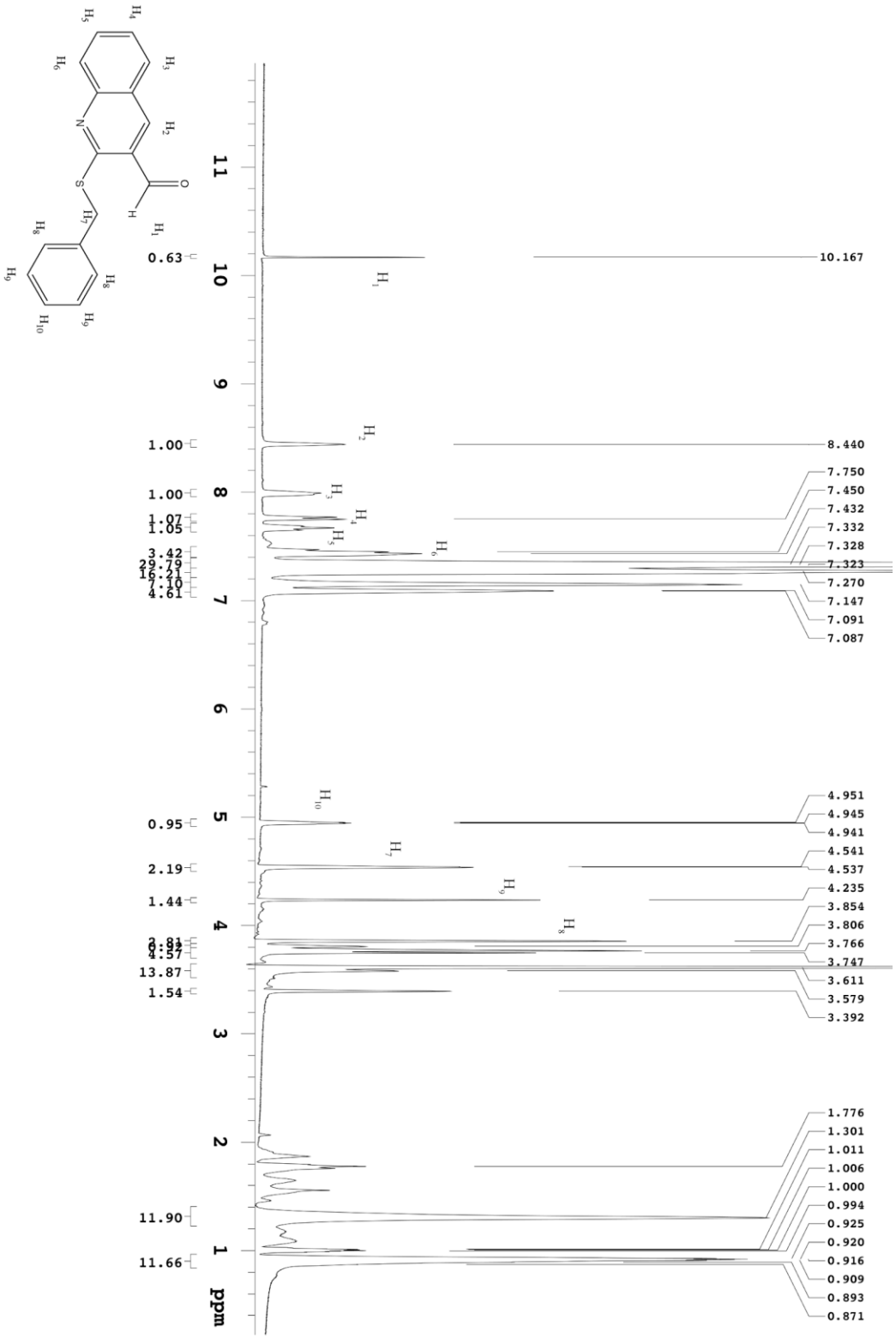
H5
H4
H6
H3
N
H2
S
O
H7
H
H1
H8
H9
H8
H10
H9
0.63
10.167
H1
11
10
9
1.00
8.440
H2
7.750
7.450
7.432
7.332
7.328
7.323
7.270
7.147
7.091
7.087
1.00
H3
1.07
H4
1.05
H5
3.42
H6
29.79
16.21
7.10
4.61
7
6
4.951
4.945
4.941
0.95
H10
5
4.541
4.537
2.19
H7
4.235
1.44
H9
3.854
3.806
3.766
3.747
H8
4
4.57
13.87
3.611
3.579
1.54
3.392
3
1.776
1.301
1.011
1.006
1.000
0.994
0.925
0.920
0.916
0.909
0.893
0.871
2
11.90
1
11.66
ppm

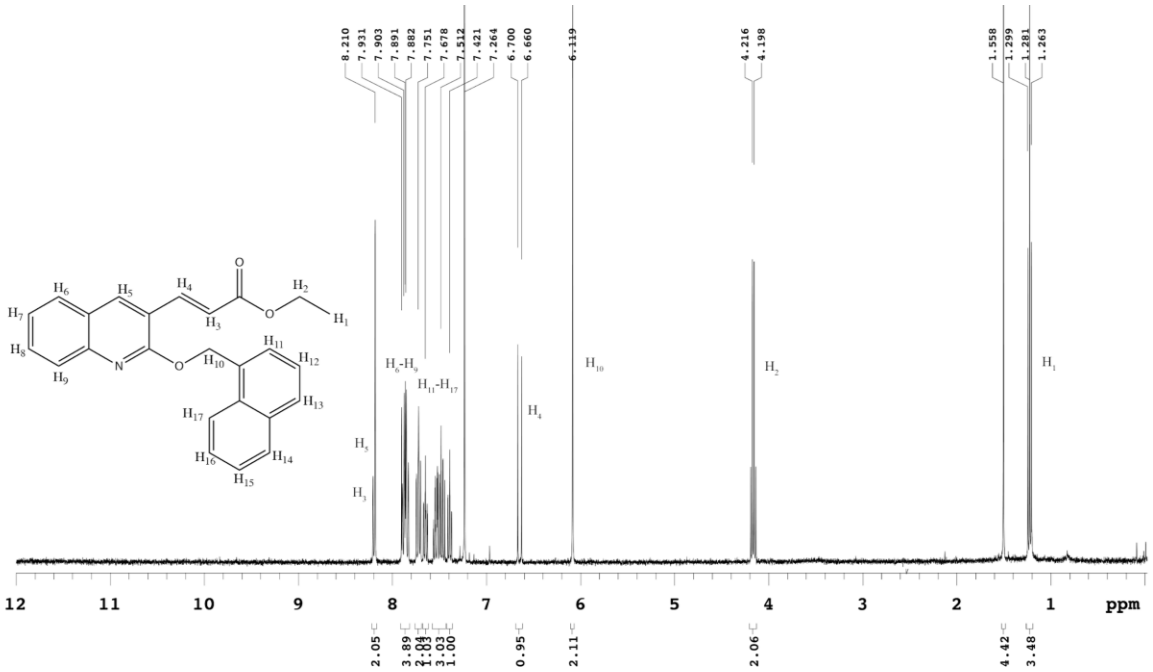
8.210
7.931
7.903
7.891
7.882
7.751
7.678
7.512
7.421
7.264
6.700
6.660
6.119
4.216
4.198
1.558
1.299
1.281
1.263
12
11
10
9
8
7
6
5
4
3
2
1
ppm
2.05
3.89
2.04
1.03
3.03
1.00
0.95
2.11
2.06
4.42
3.48

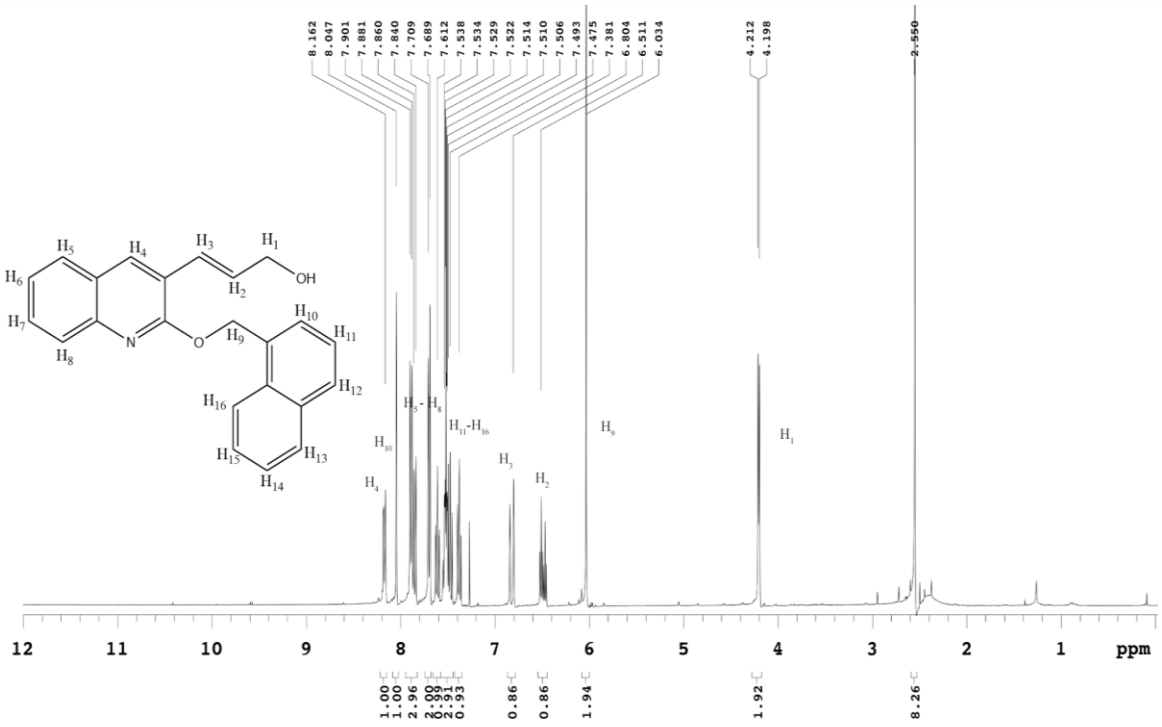
8.162
8.047
7.901
7.881
7.860
7.840
7.709
7.689
7.612
7.538
7.534
7.529
7.522
7.514
7.510
7.506
7.493
7.475
7.381
6.804
6.511
6.034
4.212
4.198
2.550
12
11
10
9
8
7
6
5
4
3
2
1
ppm
1.00
1.00
2.96
3.00
3.00
2.91
0.93
0.86
0.86
1.94
1.92
8.26

6. Acknowledgements

The author would like to express their appreciation to Dr. Amanda Wolfe, Dr. Whitney Craig, Dr. Melanie Heying, and the Wolfe Research Group, and gratefully acknowledge the financial support of the Research Corporation Cottrell Scholar Award, the GlaxoSmithKline Foundation, and the University of North Carolina Chemistry Department.

7. References

1. Pop-Vicas, A.; Strom, J.; Stanley, K.; D'Agata, E. M. C. Multidrug-Resistant Gram-Negative Bacteria among Patients Who Require Chronic Hemodialysis. *Clin. J. Am. Soc. Nephrol,* **2008**, *3*, 752–758.
2. Schwaber, M. J.; Navon-Venezia, S.; Kaye, K. S.; Ben-Ami, R.; Schwartz, D.; Carmeli, Y. Clinical and economic impact of bacteremia with extended-spectrum-beta-lactamase- producing *Enterobacter*. *Antimicrob. Agents Chemother*, **2006**, *50*, 1257–1262.
3. Koul, A.; Dendouga N.; Vergauwen K.; Molenberghs, B.; Vranckx1, L.; Willebrords, R.; Ristic, Z.; Lill, H.; Dorange, I.; Guillemont, J.; Bald, D.; Andries, K. Diarylquinolines target subunit c of mycobacterial ATP synthase. *Nat. Chem. Biol*. **2007**, *3*, 323–324.
4. He, C.; Preiss, L.; Wang, B.; Fu, L.; Wen, H.; Zhang, X.; Cui, H.; Meier, T.; Yin, D. Structural Simplification of Bedaquiline: the Discovery of 3-(4-(N,N-Dimethylaminomethyl)phenyl)quinoline-Derived Antitubercular Lead Compounds. *Chem. Med. Chem.* **2016**, *11*, 1–15.
5. Guillemont, J. E. G.; Meyer, C.; Poncelet, A.; Bourdrez, X.; Andries, K. Diarylquinolines, synthesis pathways and quantitative structure–activity relationship studies leading to the discovery of TMC207. *Future Med. Chem*. **2011**, *3*, 1345 – 1360.
6. Surase, Y. B.; Samby, K.; Amale, S. R.; Sood, R.; Purnapatre, K. P.; Pareek, P. K.; Das, B.; Nanda, K.; Kumar, S.; Verma, A. K. Identification and synthesis of novel inhibitors of mycobacterium ATP synthase. *Bioorganic Med. Chem. Lett.* **2017**, *27*, 3454-3459.
7. Preiss, L.; Langer, J. D.; Yildiz, Ö.; Eckhardt-Strelau, L.; Guillemont, J. E. G.; Koul, A.; Meier, T. Structure of the mycobacterial ATP synthase F_o rotor ring in complex with the anti-TB drug bedaquiline. *Sci. Adv.* **2015**, *1*, e1500106.
8. Andries K, Verhasselt P, Guillemont J. E. G.; Go¨hlmann, H. W. H.; Neefs, J.; Winkler, H.; Van Gestel, J.; Timmerman, P.; Zhu, M.; Lee, E.; Williams, P.; de Chaffoy, D.; Huitric, E.; Hoffner, S.; Cambau, E.; Truffot-Pernot, C.; Lounis, N.; Jarlier, V. A diarylquinoline drug active on the ATP synthase of Mycobacterium tuberculosis. *Science* **2005**, *307*, 223-7.
9. Haagsma, A. C.; Podasca, I.; Koul, A.; Guillemont, J.; Lill H.; Bald, D.; Abdillahi-Ibrahim, R.; Wagner, M. J.; Krab, K.; Vergauwen, K. Selectivity of TMC207 towards Mycobacterial ATP Synthase Compared with That towards the Eukaryotic Homologue. *Antimicrob. Agents Chemother.* **2009**, *53*, 1290–1292.
10. Balemans, W.; Vranckx, L.; Lounis, N.; Pop, O.; Guillemont, J.;Vergauwen, K.; Mol, S.; Gilissen, R.; Motte, M.; Lançois, D.; De Bolle, M.; Bonroy, K.; Lill, H.; Andries, K.; Bald, D.; Koul, A. Novel Antibiotics Targeting Respiratory ATP Synthesis in Gram-Positive Pathogenic Bacteria. *Antimicrob. Agents Chemother.* **2012**, *56*, 4131-4139.
11. Wang, X.; Zeng, Y.; Sheng, L.; Larson, P.; Liu, X.; Zou, X.; Wang, S.; Guo, K.; Ma, C.; Zhang, G.; Cui, H.; Ferguson, D. M.; Li, Y.; Zhang, J. A Cinchona Alkaloid Antibiotic That Appears To Target ATP Synthase in Streptococcus pneumoniae. *J. Med. Chem.* **2019**, *62*, 2305-2332.
12. Chandrasekhar, S.; Kiran Babu, G. S.; Mohapatra, D. K. Practical Syntheses of (2S)-R207910 and (2R)-R207910. *Eur. J. Org. Chem.* **2011**, *11*, 2057–2061.
13. Haagsma, A. C.; Podasca, I.; Koul, A.; Andries, K.; Guillemont, J.; Lill H.; Bald, D. Probing the Interaction of the Diarylquinoline TMC207 with Its Target Mycobacterial ATP Synthase. *PLOS ONE*, **2011**, *8*, e23575.